

Article

# Ab initio Quantum-Chemical Calculations and Spectroscopic Studies of the Intramolecular $\pi$ -Type Hydrogen Bonding in Small Cyclic Molecules

Esther J. Ocola<sup>1,2</sup> and Jaan Laane<sup>1,2,\*</sup>

<sup>1</sup> Department of Chemistry, Texas A&M University, College Station, TX 77843-3255, USA

<sup>2</sup> Institute for Quantum Science and Engineering, Texas A&M University, College Station, TX 77843-4242, USA

\* Correspondence: laane@chem.tamu.edu

**How To Cite:** Ocola, E.J.; Laane, J. Ab initio Quantum-Chemical Calculations and Spectroscopic Studies of the Intramolecular  $\pi$ -Type Hydrogen Bonding in Small Cyclic Molecules. *Photochemistry and Spectroscopy* **2025**, *1*(1), 2.

Received: 17 September 2025

Revised: 11 October 2025

Accepted: 14 October 2025

Published: 20 October 2025

**Abstract:** Ab initio single-point energy computations at the CCSD(T)/aug-cc-pVTZ level have been carried out on nine molecules possessing intramolecular  $\pi$ -type hydrogen bonding. These computations were done using the calculated geometrical structures from CCSD/cc-pVTZ optimizations. The outcome has been analyzed together with previous spectroscopic and theoretical work. Results are presented for 3-cyclopenten-1-ol, 2-indanol, 2-cyclopenten-1-ol, 2-cyclohexen-1-ol, 3-cyclohexen-1-ol, and 2-cyclopropen-1-ol with O–H $\cdots\pi$ (C=C) bonding. Results for 3-cyclopenten-1-amine and 2-cyclopropen-1-amine with N–H $\cdots\pi$ (C=C) bonding and for 2-cyclopropen-1-thiol with S–H $\cdots\pi$ (C=C) bonding are also discussed. For each molecule, the conformer with a weak intramolecular  $\pi$ -type hydrogen bond was found to be the global minimum, with the exception of 2-cyclopropen-1-thiol. In this case, the S–H $\cdots\pi$  bonded conformer is higher in energy, indicating a weaker interaction. The hydrogen bonded conformers for the cyclic alcohols typically have conformational energies about 250 to 350 cm<sup>−1</sup> lower than the other conformers. For the amines the lowering is about half of that. The infrared and Raman spectra for several molecules in the O–H stretching region show hydrogen bonded conformers to be at the lowest frequencies. The calculated potential energy surfaces for six of the molecules are also presented.

**Keywords:**  $\pi$ -type intramolecular hydrogen bonding; Raman spectroscopy; infrared spectroscopy; conformations; potential energy surface; CCSD(T)/aug-cc-pVTZ

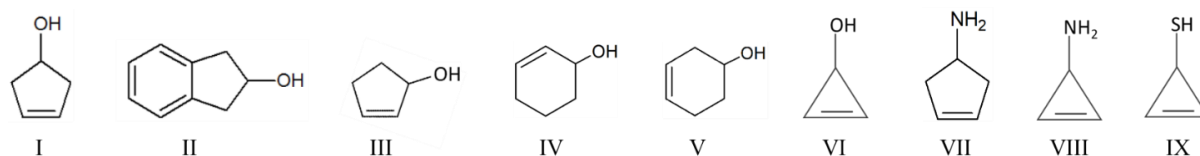
## 1. Introduction

Hydrogen bonding occurs in simple molecules, crystals, supramolecular systems and biological molecules [1–65]. The hydrogen bonds can be intermolecular [8–22,58] or intramolecular [12–65]. Weak intramolecular hydrogen bonded interactions are often of great interest [13,34–65]. In particular, the intramolecular  $\pi$ -type hydrogen bonding between C=C double bonds with OH groups [13,35–58], NH<sub>2</sub> groups [51,56–63], and SH groups [57,61,64,65] have been studied over the years by several research groups.

For more than 50 years the Laane research group has been engaged in the investigation of the conformational dynamics of small ring molecules as well as internal rotations [56,66–74]. A research area on which we have focused involves the spectroscopic and computational investigation of weak intramolecular  $\pi$ -type hydrogen bonding between OH [49–57], NH<sub>2</sub> [51,56,57,59] and SH [57] groups and C=C double bonds in molecules, namely X–H $\cdots\pi$ (C=C), where X=O, N or S. Infrared and Raman spectroscopy as well as a variety of computational methods have been utilized [49–57,59].



Among the molecules which we have studied are 3-cyclopenten-1-ol (I) [49–51], 2-indanol (II) [52], 2-cyclopenten-1-ol (III) [51,53], 2-cyclohexen-1-ol (IV) [51,54], 3-cyclohexen-1-ol (V) [55] and 2-cyclopropen-1-ol (VI) [57], all of which possess weak intramolecular O–H $\cdots\pi$  hydrogen bonds. 3-Cyclopenten-1-amine (VII) [51,59], 2-cyclopropen-1-amine (VIII) [57], which possess weak intramolecular N–H $\cdots\pi$  hydrogen bonds, and 2-cyclopropen-1-thiol (IX) [57], which possesses a weak intramolecular S–H $\cdots\pi$  hydrogen bond have also been investigated. The molecules I to IX are shown in the scheme below.



In previous work, we performed CCSD/cc-pVTZ and MP2/cc-pVTZ geometrical structure optimizations and energy calculations for each of the molecules I–IX. However, the calculated relative energy order for the conformers from CCSD computations did not agree with those from the MP2 ones in every case. Therefore, in order to provide a homogeneous labelling of the conformers of the molecules according to their relative energies, we decided to utilize the order resulting from our newly done single-point energy CCSD(T)/aug-cc-pVTZ computations. The optimized geometrical structures used for the input for the new calculations were derived from CCSD/cc-pVTZ computations which were previously carried out [51,53–55,57,59], with the exception of 2-indanol, which comes from our present work. CCSD(T) stands for coupled-cluster singles, doubles and perturbative triples and CCSD stands for coupled cluster singles and doubles. Aug-cc-pVTZ is the augmented version of the Dunning’s correlation-consistent basis set, polarized, triple-zeta basis set (cc-pVTZ). As a result, the order of the calculated relative energies and the labelling of the conformers have been modified for several molecules.

The present paper presents the experimental results and the previously calculated potential energy surfaces with the updated labelling for each conformer of the molecules. We also present tables comparing of the single-point energy calculations results from the CCSD(T)/aug-cc-pVTZ computations with the results of the energy calculations from the full geometry optimizations carried out by CCSD/cc-pVTZ and MP2/cc-pVTZ computations [49,51–55,57,59]. We also present calculated geometrical structural parameters for the conformers of each molecule along with the experimental OH, NH and C=C stretching vibrational frequencies wherever available.

## 2. Materials and Methods

### 2.1. Computations

The Gaussian16 program [75] was used for the theoretical computations, and the GaussView 6.1.1 program [76] was used to visualize the structures. Maple (2015, 2019.2) software [77] was used to attain the potential energy surfaces (PES).

The definitions for the ring-puckering angle, ring-puckering ( $\chi$ ), ring-twisting angle as well as (O, S)H and NH<sub>2</sub> internal rotational coordinates are shown in Figure 1.

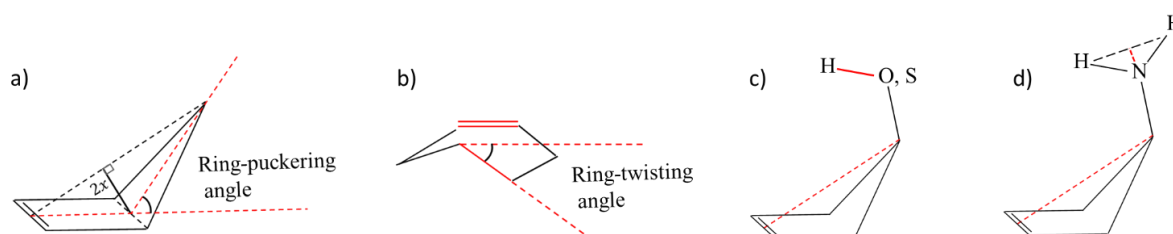


**Figure 1.** (a) Definition of the ring-puckering angle. The ring-puckering coordinate  $\chi$  is also shown. (b) Definition of the ring-twisting angle of a six-membered ring. The ring-twisting angle is the dihedral angle formed between the double bond and the C–C bond indicated in red. (c) The (O, S)H internal rotation angle is measured by the dihedral angle formed by the dashed line and the (O, S)–H bond. (d) The NH<sub>2</sub> internal rotation angle is measured by the dihedral angle formed by the two red dashed lines, where one of them links the N atom with the midpoint of the black dashed line.

## 2.2. Experimental

### 2.2.1. Infrared Spectra

The infrared (IR) spectra were previously obtained with a 4.2 m Infrared Industries long path multireflection cell with KBr windows for 3-cyclopenten-1-ol [50,51] and with a 10 cm mid-infrared cell with KBr windows for 2-cyclopenten-1-ol [53], 2-cyclohexen-1-ol [54], 3-cyclohexen-1-ol [55] and 3-cyclopenten-1-amine [59]. The samples were purified by trap-to-trap distillation. The vapor-phase IR spectra were recorded using a Bruker Vertex 70 instrument, which was purged by a stream of dry nitrogen gas.

### 2.2.2. Raman Spectra

The Raman spectra of vapor samples of 3-cyclopenten-1-ol (I) [50,51], 2-cyclohexen-1-ol (IV) [54], 3-cyclohexen-1-ol [(V) 55] and 3-cyclopenten-1-amine (VII) [59] were collected with a Jobin Yvon U-1000 spectrometer equipped with a charge coupled device (CCD) detector. A Coherent Verdi V10 Nd:YAG laser operating at 532 nm was the excitation source. A heatable Raman cell was used [78,79]. Figure 2a shows an image of the Raman cell in front of the lens of the equipment at the entrance of the double monochromator of the spectrometer. Figure 2b,c show the Raman cell unwrapped and wrapped with a heating tape, respectively.

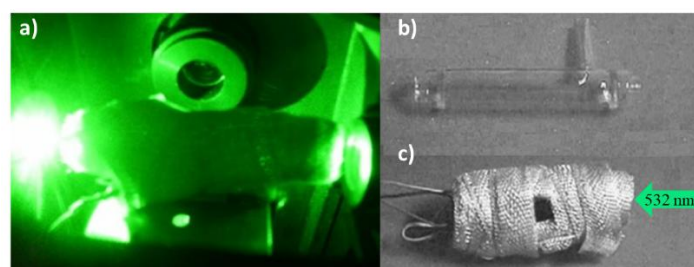


**Figure 2.** (a) Wrapped Raman cell in front of the lens of the instrument at the entrance of the double monochromator of the spectrometer. (b) Glass Raman cell into which the sample was introduced for purification and vaporization. (c) Wrapped Raman cell with heatable tape.

All of the IR and Raman spectra have been previously reported [50,51,53–55,59].

## 3. Results

### 3.1. Unsaturated 5-Membered Ring Molecules with Weak Intramolecular Hydrogen Bonding

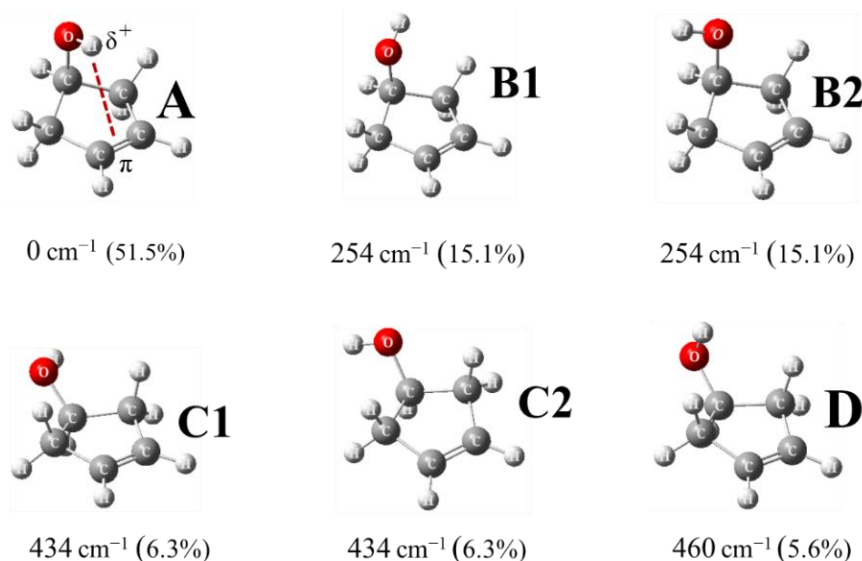
#### 3.1.1. 3-Cyclopenten-1-ol (I)

3-Cyclopenten-1-ol possesses six conformers which can interconvert into each other through ring-puckering and OH internal rotational motions. Conformer **A** in Figure 3 possesses the  $\pi$  type hydrogen bonding and is of lowest energy. Conformers **B1** and **B2** are mirror images of each other. Similarly, conformers **C1** and **C2** are also mirror images. Figure 4a shows the calculated potential energy surface (PES) from MP2/6-31+G(d,p) computations for this molecule [49]. For simplification, the minima for **B2** and **C2** are not shown since they have the same energy as their mirror images.

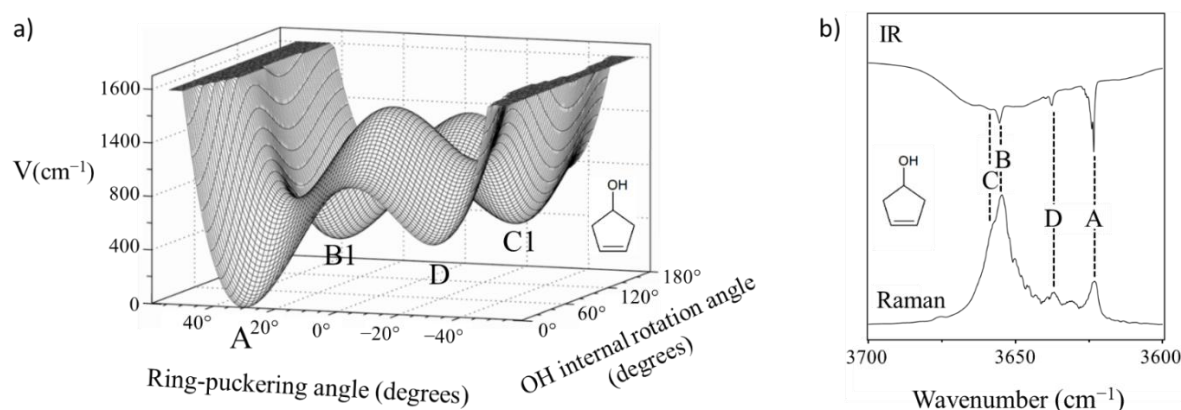
The conformer with lowest energy of 3-cyclopenten-1-ol is **A** which lies  $254\text{ cm}^{-1}$  (0.73 kcal/mol) to  $460\text{ cm}^{-1}$  (1.32 kcal/mol) lower in energy than the other conformers according to CCSD(T)/aug-cc-pVTZ computations. This conformer has a calculated population abundance of 51.5% in its vapor state at room temperature. Table 1 presents the calculated relative energies of 3-cyclopenten-1-ol from ab initio CCSD(T)/aug-cc-pVTZ, CCSD/cc-pVTZ and MP2/cc-pVTZ computations. This table also shows the calculated distance from the hydrogen atom attached to the oxygen to the center of the double bond (Å). The ring-puckering angle (degrees) and the OH internal rotation angle (degrees) for each conformer are also shown.

Conformer **A** is the only conformer of 3-cyclopenten-1-ol which possesses the weak intramolecular O–H $\cdots\pi$  hydrogen bond, and this is responsible for lowering its conformational energy. This conformer has a weakened O–H bond due to the intramolecular interaction and has a sharp IR peak for the vapor phase molecule for its O–H stretch at  $3623\text{ cm}^{-1}$  as shown in Figure 4b. This vibrational frequency is 14 to  $35\text{ cm}^{-1}$  lower than those of the other conformers listed in Table 1 along with the C=C stretching frequencies for all of the conformers. [50,51]. All of the IR peaks were confirmed by vapor-phase Raman spectroscopy at  $186^\circ$  [50,51].

The observed double bond C=C stretching frequency for conformer **A** at  $1607\text{ cm}^{-1}$  is lower than the frequencies for the other conformers reflecting a slight weakening of the C=C bond resulting from the  $\pi$  bonding [50,51]. The calculated hydrogen bond O–H $\cdots\pi$  angle in degrees is  $99.9^\circ$  from CCSD/cc-pVTZ and  $101.6^\circ$  from MP2/cc-pVTZ computations [55].



**Figure 3.** Calculated geometrical structures of the six conformers of 3-cyclopenten-1-ol from CCSD/cc-pVTZ computations. The relative energies and vapor-phase populations (in parentheses) at  $25^\circ\text{C}$  for each conformer are from CCSD(T)/aug-cc-pVTZ computations.

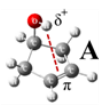


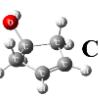
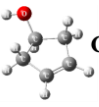
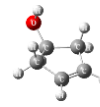


**Figure 4.** (a) Calculated PES from MP2/6-31+G(d,p) computations for 3-cyclopenten-1-ol. (b) Vapor-phase infrared spectrum at  $25^\circ\text{C}$  and Raman spectrum at  $186^\circ\text{C}$  of 3-cyclopenten-1-ol in the OH stretching region.

**Table 1.** Calculated relative energies and selected geometrical structural parameters of the conformers of 3-cyclopenten-1-ol (I) and observed OH and C=C bonds vibrational frequencies in the vapor phase.

Conformers Labelled According to the CCSD(T)/aug-cc-pVTZ Calculated Energies							
Method of calculation		Relative energy ( $\text{cm}^{-1}$ )					
CCSD(T)/aug-cc-pVTZ	0	254	254	434	434	460	This work
CCSD/cc-pVTZ	0	301	301	402	402	411	[51]
MP2/cc-pVTZ	0	401	401	560	560	564	[49]

Table 1. Cont.

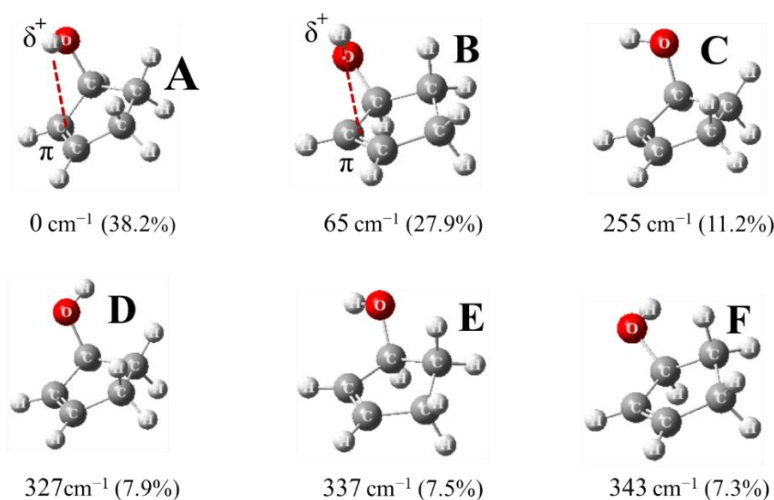
Conformers Labelled According to the CCSD(T)/aug-cc-pVTZ Calculated Energies							
							Reference
	Hydrogen attached to the oxygen distance to the center of the double bond (Å).						
CCSD/cc-pVTZ	2.744	3.664	3.664	4.109	4.109	3.701	This work
MP2/cc-pVTZ	2.672	3.622	3.622	4.105	4.105	3.715	This work
	Ring-puckering angle (degrees)						
CCSD/cc-pVTZ	28.0°	22.1°	22.1°	−26.8°	−26.8°	−28.0°	[51]
MP2/cc-pVTZ	30.2°	24.3°	24.3°	−29.5°	−29.5°	−30.6°	[49]
	OH internal rotation angle (degrees)						
CCSD/cc-pVTZ	0°	117.4°	−117.4°	130.0°	−130.0°	0°	This work
MP2/cc-pVTZ	0°	116.7°	−116.7°	130.1°	−130.1°	0°	This work
Observed	Vibrational frequencies (cm <sup>−1</sup> )						
OH stretch	3623	3655	3655	3659	3659	3638	[50,51]
C=C stretch	1607	1620	1620	1615	1615	1609	[50,51]

### 3.1.2. 2-Cyclopenten-1-ol (III)

2-Cyclopenten-1-ol possesses six conformers which can interconvert into each other by ring-puckering and OH internal rotational motions. Figure 5 shows the calculated geometrical structures of the conformers. Figure 6a shows the calculated potential energy surface (PES) from MP2/cc-pVTZ computations for this molecule [53].

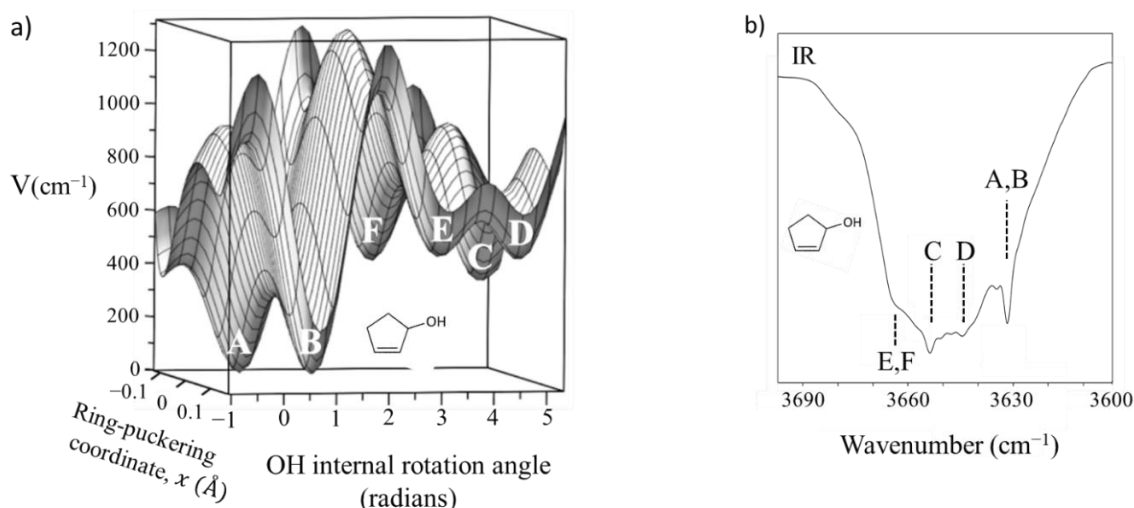
Conformers **A** and **B** possess weak intramolecular O–H··· $\pi$  hydrogen bonds. Conformer **A** lies 255 cm<sup>−1</sup> (0.73 kcal/mol) to 343 cm<sup>−1</sup> (0.98 kcal/mol) lower in energy than the conformers with no intramolecular hydrogen bonding, whereas conformer **B** lies 190 cm<sup>−1</sup> (0.54 kcal/mol) to 278 cm<sup>−1</sup> (0.79 kcal/mol) lower in energy than the conformers with no intramolecular hydrogen bonding according to CCSD(T)/aug-cc-pVTZ computations. The calculated populations for the two conformers are 38% for **A** and 30% for **B** for their vapor states at room temperature. Table 2 presents the calculated relative energies of 2-cyclopenten-1-ol from ab initio CCSD(T)/aug-cc-pVTZ, CCSD/cc-pVTZ and MP2/cc-pVTZ computations. The table also presents calculated geometrical structural parameters of 2-cyclopenten-1-ol.

Conformers **A** and **B**, which possess the weak intramolecular O–H··· $\pi$  hydrogen bonds, together show a sharp IR peak at 3632 cm<sup>−1</sup> for their O–H stretching vibrations. This vibrational frequency is 12 to 32 cm<sup>−1</sup> lower than those of the other conformers without the hydrogen bonding as can also be seen in Table 2. Figure 6b shows this for 2-cyclopenten-1-ol in the OH stretching region. The observed double bond C=C stretching frequency for conformer **A** is at 1609 cm<sup>−1</sup> [53]. The calculated hydrogen bond O–H··· $\pi$  angle for conformer **A** in degrees is 86.6° from CCSD/cc-pVTZ and 88.2° from MP2/cc-pVTZ computations [55].



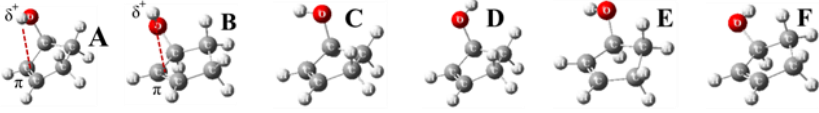
**Figure 5.** Calculated geometrical structures of the six conformers of 2-cyclopenten-1-ol from CCSD/cc-pVTZ computations. The calculated relative energies and vapor-phase populations (in parentheses) at 25 °C are from CCSD(T)/aug-cc-pVTZ computations.





**Figure 6.** (a) Calculated PES from MP2/cc-pVTZ computations for 2-cyclopenten-1-ol. (b) Vapor-phase infrared spectrum at 25 °C in the OH stretching region.

**Table 2.** Calculated relative energies and selected geometrical structural parameters of the conformers of 2-cyclopenten-1-ol (III) and observed OH and C=C stretch vibrational frequencies in the vapor phase.

Conformers Labelled According to the CCSD(T)/aug-cc-pVTZ Calculated Energies							
							Reference
Method of calculation	Relative energy (cm <sup>-1</sup> )						
CCSD(T)/aug-cc-pVTZ	0	65	255	327	337	343	This work
CCSD/cc-pVTZ	0	9	293	304	308	361	[53]
MP2/cc-pVTZ	0	89	308	406	406	409	[51,53]
	Hydrogen atom on the oxygen distance to the center of the double bond (Å)						
CCSD/cc-pVTZ	2.682	3.001	3.019	3.554	3.335	3.680	[53]
MP2/cc-pVTZ	2.631	2.997	2.972	3.534	3.337	3.678	[51]
	Ring-puckering angle (degrees)						
CCSD/cc-pVTZ	-21.1°	22.5°	-23.1°	22.8°	23.7°	-22.8°	[53]
MP2/cc-pVTZ	-23.6°	24.3°	-25.7°	24.4°	25.6°	-25.3°	[51,53]
	OH internal rotation angle (degrees)						
CCSD/cc-pVTZ	24.8°	39.2°	284.3°	269.0°	172.3°	166.9°	[53]
MP2/cc-pVTZ	22.6°	38.7°	286.4°	268.6°	172.3°	166.9°	[53]
Observed	Vibrational frequencies (cm <sup>-1</sup> )						
OH stretch	3632	3632	3654	3644	3664	3664	[53]
C=C stretch	1609	Not reported	Not reported	Not reported	Not reported	Not reported	[53]

### 3.1.3. 3-Cyclopenten-1-amine (VII)

3-Cyclopenten-1-amine possesses six conformers which can interconvert into each other by ring-puckering and NH<sub>2</sub> internal rotation. Conformers **A1** and **A2** are mirror images of each other as are **C1** and **C2**. All six conformers of the molecule are illustrated in Figure 7. The calculated potential energy surface (PES) from MP2/cc-pVTZ computations is shown in Figure 8a [59].

Conformers **A1** and **A2** possess weak intramolecular N–H···π hydrogen bonds. These two conformers lie 128 cm<sup>-1</sup> (0.37 kcal/mol) to 200 cm<sup>-1</sup> (0.57 kcal/mol) lower in energy than the other conformers according to CCSD(T)/aug-cc-pVTZ computations. The calculated relative population of conformers **A1** and **A2** is 26.9% in their vapor state at room temperature. Table 3 presents the calculated relative energies of 3-cyclopenten-1-amine from ab initio CCSD(T)/aug-cc-pVTZ, CCSD/cc-pVTZ and MP2/cc-pVTZ computations. This table also presents calculated selected geometrical structural parameters.

Conformers **A1** and **A2** together have a sharp IR peak resulting from the NH<sub>2</sub> antisymmetric stretch at 3391 cm<sup>-1</sup>. This frequency is 5 to 12 cm<sup>-1</sup> lower than the those of the other conformers as shown in Table 3 [59]. As

shown in Figure 8b, all of the IR peaks were confirmed by vapor-phase Raman spectroscopy at 116 °C [59]. The observed double bond C=C stretching frequency for conformers **A1** and **A2** is 1613 cm<sup>-1</sup> [59]. The calculated hydrogen bond N–H··· $\pi$  angle in degrees is 96.1° from CCSD/cc-pVTZ and 97.5° from MP2/cc-pVTZ computations.

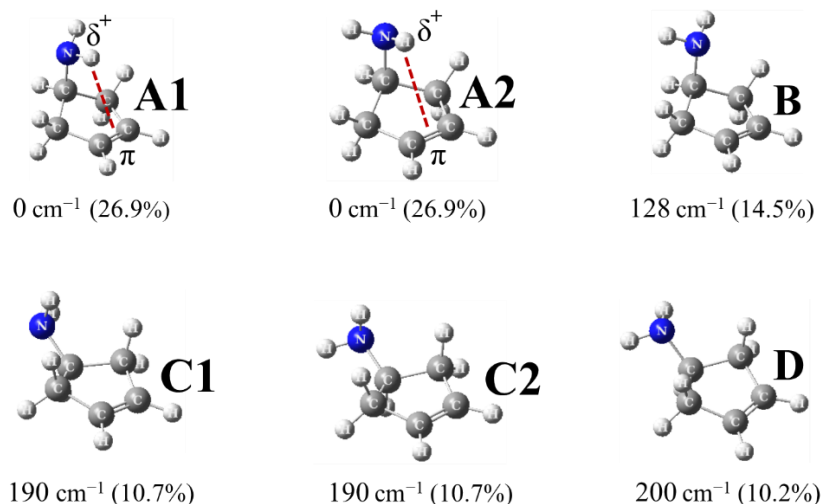


**Figure 7.** Calculated geometrical structures of the six conformers of 3-cyclopenten-1-amine from CCSD/cc-pVTZ computations. The relative energies and vapor phase populations at 25 °C per conformer are from CCSD(T)/aug-cc-pVTZ computations. The relative populations are shown in parentheses.

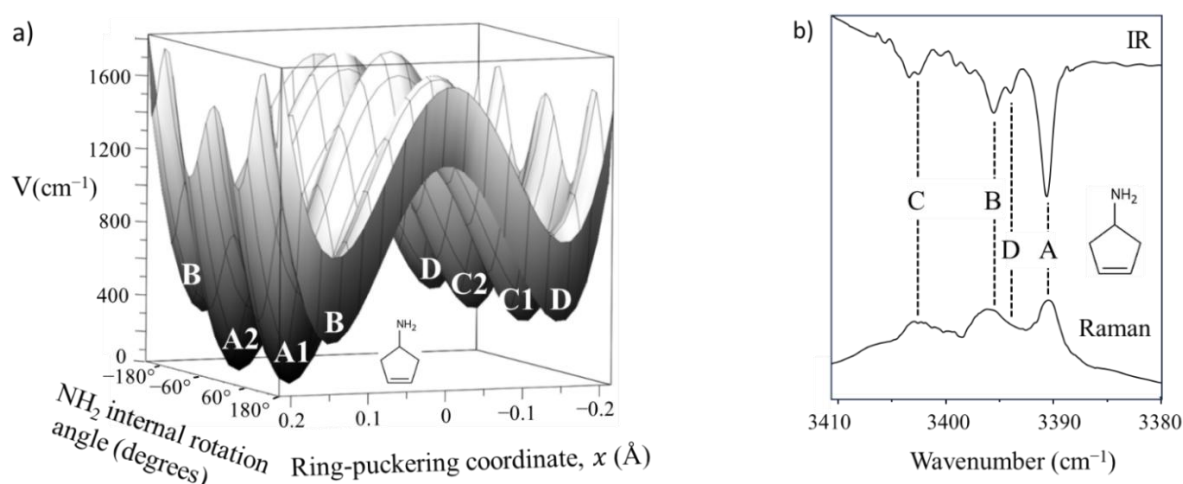


**Figure 8.** (a) Calculated PES from MP2/cc-pVTZ computations for 3-cyclopenten-1-amine. (b) Vapor infrared spectrum at 25 °C and Raman spectrum at 116 °C in the NH<sub>2</sub> antisymmetric stretching region.

**Table 3.** Calculated relative energies and selected geometrical structural parameters of the conformers of 3-cyclopenten-1-amine (VII) and observed NH<sub>2</sub> and C=C stretch vibrational frequencies in the vapor phase.

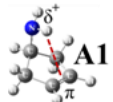
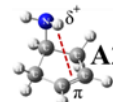
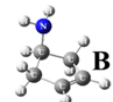
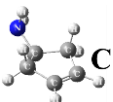
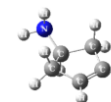
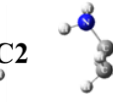
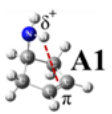
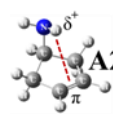
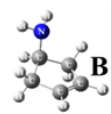
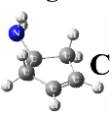
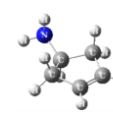
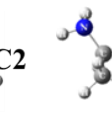
Conformers Labelled According to the CCSD(T)/aug-cc-pVTZ Calculated Energies							
							Reference
Method of calculation	Relative energy (cm <sup>-1</sup> )						
CCSD(T)/aug-cc-pVTZ	0	0	128	190	190	200	This work
CCSD/cc-pVTZ	0	0	197	165	165	188	[59]
MP2/cc-pVTZ	0	0	284	315	315	336	[51,59]

Table 3. Cont.

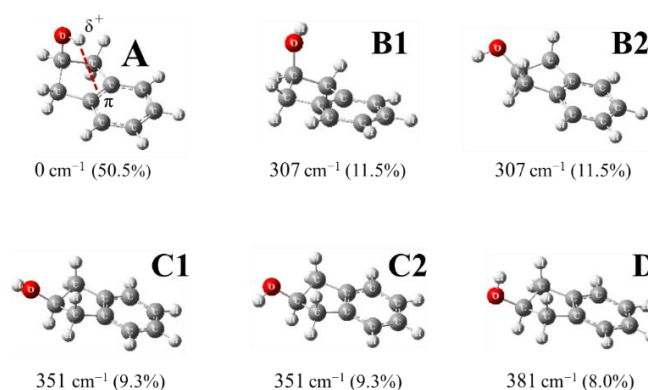
Conformers Labelled According to the CCSD(T)/aug-cc-pVTZ Calculated Energies							
	 <b>A1</b>	 <b>A2</b>	 <b>B</b>	 <b>C1</b>	 <b>C2</b>	 <b>D</b>	Reference
	Hydrogen attached to the nitrogen distance to the center of the double bond (Å)						
CCSD/cc-pVTZ <sup>a</sup>	2.850	3.765	3.798	3.780	4.223	4.173	[59]
MP2/cc-pVTZ <sup>a</sup>	2.773	3.715	3.750	3.793	4.217	4.168	[51]
CCSD/cc-pVTZ <sup>b</sup>	3.765	2.850	3.798	4.223	3.780	4.173	[59]
MP2/cc-pVTZ <sup>b</sup>	3.715	2.773	3.750	4.217	3.793	4.168	[51]
	Ring-puckering angle (degrees)						
CCSD/cc-pVTZ	26.3°	26.3°	20.5°	−26.8°	−26.8°	−25.9°	[59]
MP2/cc-pVTZ	28.7°	28.7°	23.0°	−29.3°	−29.3°	−28.5°	[51]
	NH <sub>2</sub> internal rotation angle (degrees)						
CCSD/cc-pVTZ	59.0°	−59.0°	180°	67.9°	−67.9°	180°	[59]
MP2/cc-pVTZ	58.6°	−58.6°	180°	68.4°	−68.4°	180°	This work
Observed	Vibrational frequencies (cm <sup>−1</sup> )						
NH <sub>2</sub> antisymmetric stretch	3391	3391	3396	3403	3403	3394	[59]
NH <sub>2</sub> symmetric stretch	3329	3329	3335	3335	3335	3335	[59]
C=C stretch	1613	1613	1613	1599	1599	1603	[59]

### 3.1.4. 2-Indanol (II)

2-Indanol possesses six conformers which can interconvert into each other by ring-puckering and OH internal rotation. Conformers **B1** and **B2** shown in Figure 9 are mirror images of each other as are conformers **C1** and **C2**. Figure 10a shows the calculated potential energy surface (PES) from MP2/cc-pVTZ computations [52]. For simplification, the minima for **B2** and **C2** are not shown since they have same energies as their mirror images.

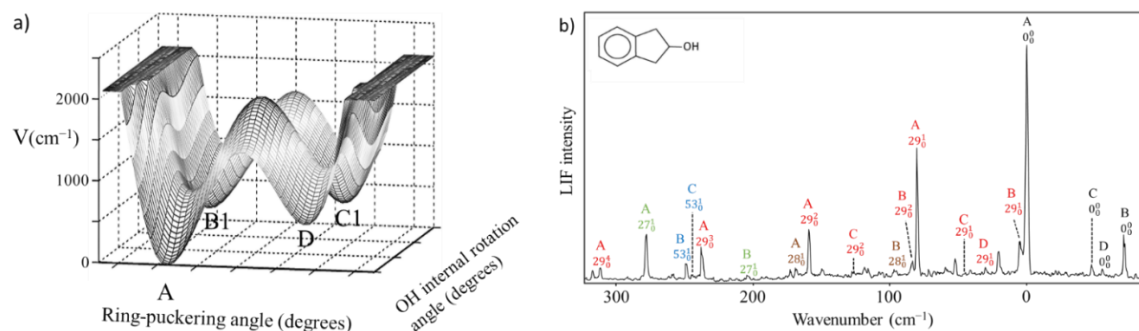
The conformer with lowest energy of 2-indanol is **A** which lies 307 cm<sup>−1</sup> (0.88 kcal/mol) to 381 cm<sup>−1</sup> (1.09 kcal/mol) lower in energy than the other conformers according to CCSD(T)/aug-cc-pVTZ computations. This conformer has a calculated abundance of 50.5% at room temperature. Table 4 presents the calculated relative energies of 2-indanol from ab initio CCSD(T)/aug-cc-pVTZ, CCSD/cc-pVTZ and MP2/cc-pVTZ computations. This table also presents calculated structural parameters of 2-indanol.

Only conformer **A** of 2-indanol possesses the weak intramolecular O–H⋯π hydrogen bonding and is thus lowest in conformational energy. This conformer also has a weakened O–H bond due to the intramolecular interaction. Conformer **A** has the most intense bands in the vapor-phase laser-induced fluorescence (LIF) excitation spectrum of 2-indanol at 90 °C [52]. Figure 10b shows the LIF for 2-indanol where the conformers have been relabeled alphabetically according to their relative calculated energies. It can be seen in the figure that the intensities of the pure electronic transitions 0<sub>0</sub><sup>0</sup> of the conformers decrease as the relative energies of the conformers increase.



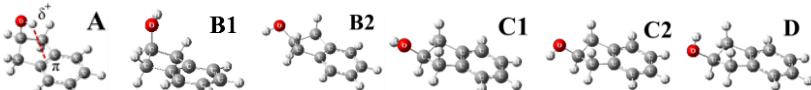
**Figure 9.** Calculated geometrical structures of the six conformers of 2-indanol from CCSD/cc-pVTZ computations. The relative energies and estimated vapor-phase populations (in parentheses) at 25 °C per conformer are from CCSD(T)/aug-cc-pVTZ computations.





**Figure 10.** (a) Calculated PES from MP2/cc-pVTZ computations for 2-indanol. (b) Vapor laser-induced fluorescence excitation spectrum at 90 °C. The  $0_0^0$  bands are shown in black, the quantum state transitions of the ring-puckering ( $\nu_{29}$ ) are shown in red, of the OH-internal rotation ( $\nu_{53}$ ) are shown in blue, of the ring-angle bending ( $\nu_{27}$ ) are shown in green and of the 2-indanol flapping ( $\nu_{28}$ ) are shown in brown.

**Table 4.** Calculated relative energies and selected geometrical structural parameters of the conformers of 2-indanol (II).

Conformers Labelled According to the CCSD(T)/aug-cc-pVTZ Calculated Energies							
							Reference
Method of calculation	Relative energy ( $\text{cm}^{-1}$ )						
CCSD(T)/aug-cc-pVTZ	0	307	307	321	351	381	This work
CCSD/cc-pVTZ	0	335	335	292	292	306	This work
MP2/cc-pVTZ	0	440	440	469	469	483	[52]
	Hydrogen atom on the oxygen distance to the center of the double bond (Å)						
CCSD/cc-pVTZ	2.656	3.562	3.562	4.118	4.118	3.738	This work
MP2/cc-pVTZ	2.579	3.513	3.513	4.110	4.110	3.744	This work
	Ring-puckering angle (degrees)						
CCSD/cc-pVTZ	33.2°	29.0°	29.0°	−32.8°	−32.8°	−33.0°	This work
MP2/cc-pVTZ	35.4°	31.1°	31.1°	−34.9°	−34.9°	−35.1°	[52]
	OH internal rotation angle (degrees)						
CCSD/cc-pVTZ	0°	115.6°	−115.6°	131.8°	−131.8°	0°	This work
MP2/cc-pVTZ	0°	114.9°	−114.9°	132.2°	−132.2°	0°	[52]

The calculated hydrogen bond  $\text{O}-\text{H}\cdots\pi$  angle in degrees is 101.2° from CCSD/cc-pVTZ and 102.9° from MP2/cc-pVTZ computations [55].

### 3.2. Unsaturated 6-Membered Ring Molecules with a Weak Intramolecular Hydrogen Bonding

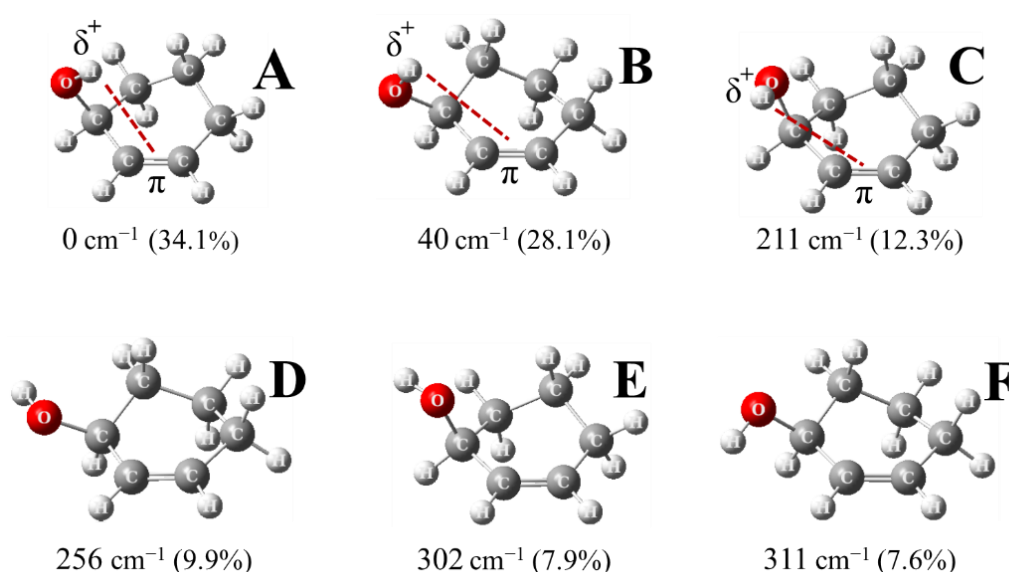
#### 3.2.1. 2-Cyclohexen-1-ol (IV)

2-Cyclohexen-1-ol possesses six conformers which can interconvert into each other by ring-twisting and OH internal rotation. Figure 11 shows the calculated geometric structures of the conformers, and Figure 12a shows the calculated potential energy surface (PES) from MP2/cc-pVTZ computations [54].

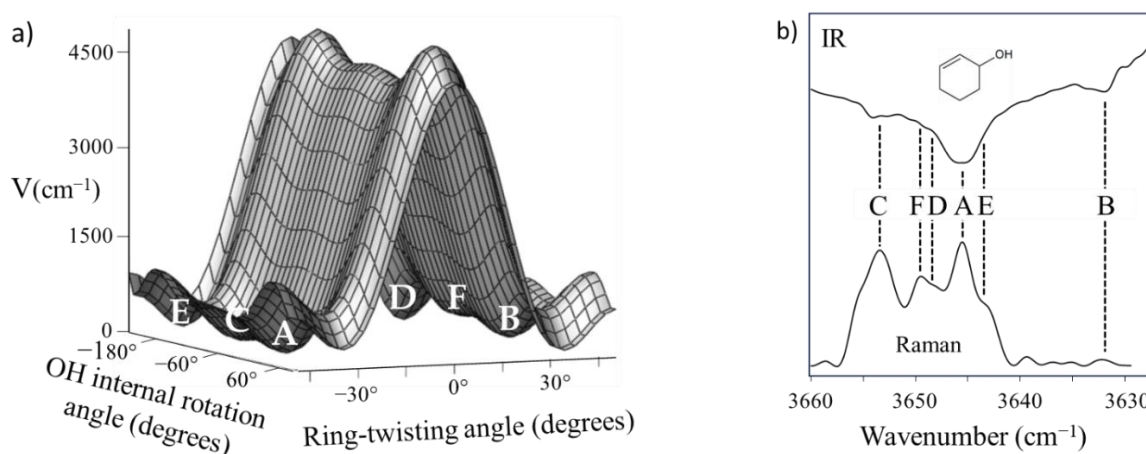
Conformers **A**, **B** and **C** all possess weak intramolecular  $\text{O}-\text{H}\cdots\pi$  hydrogen bonds. These three conformers have calculated populations of 34% for **A**, 28% for **B** and 12% for **C** in their vapor state at room temperature. Conformer **A** lies 256  $\text{cm}^{-1}$  (0.73 kcal/mol) to 311  $\text{cm}^{-1}$  (0.89 kcal/mol) lower in energy than the conformers with no hydrogen bonding according to CCSD(T)/aug-cc-pVTZ computations. Table 5 presents the calculated relative energies of 2-cyclohexen-1-ol from ab initio CCSD(T)/aug-cc-pVTZ, CCSD/cc-pVTZ and MP2/cc-pVTZ computations. This table also presents calculated geometrical structural parameters.

The O-H stretching frequencies for the conformers are also listed in Table 5, and Figure 12b shows the recorded IR and Raman spectra. Conformer **A** has the strongest IR peak, and conformer **B**, which also has an intramolecular  $\text{O}-\text{H}\cdots\pi$  hydrogen bond, has the lowest frequency [54]. The observed double bond  $\text{C}=\text{C}$  stretching frequency for conformer **A** is 1652  $\text{cm}^{-1}$  and is slightly lower than for the other conformers [54]. The calculated

hydrogen bond O–H $\cdots\pi$  angle of conformer **A** in degrees is 86.9° from CCSD/cc-pVTZ and 88.2° from MP2/cc-pVTZ computations [55].



**Figure 11.** Calculated geometrical structures of the six conformers of 2-cyclohexen-1-ol from CCSD/cc-pVTZ computations. The relative energies and vapor-phase populations (in parentheses) at 25 °C for each conformer are from CCSD(T)/aug-cc-pVTZ computations.

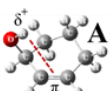
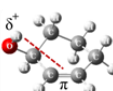
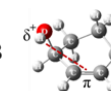
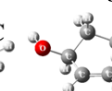
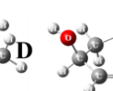
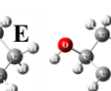


**Figure 12.** (a) Calculated PES from MP2/cc-pVTZ computations for 2-cyclohexen-1-ol. (b) Vapor-phase infrared spectrum at 100 °C and Raman spectrum at 168 °C in the OH stretch region.

**Table 5.** Calculated relative energies and selected geometrical structural parameters of the conformers of 2-cyclohexen-1-ol (IV) and observed OH and C=C stretch vibrational frequencies in the vapor phase.

Conformers Labelled According to the CCSD(T)/aug-cc-pVTZ Calculated Energies							
Method of calculation		Relative energy (cm <sup>-1</sup> )					
CCSD(T)/aug-cc-pVTZ	0	40	211	256	302	311	This work
CCSD/cc-pVTZ	9	0	208	232	284	304	[54]
MP2/cc-pVTZ	0	72	204	323	316	401	[51,54]
Hydrogen atom on the oxygen distance to the center of the double bond (Å),							
CCSD/cc-pVTZ	2.765	3.034	2.949	3.731	3.656	3.239	This work
MP2/cc-pVTZ	2.737	3.015	2.906	3.725	3.651	3.227	[51,54]

Table 5. Cont.

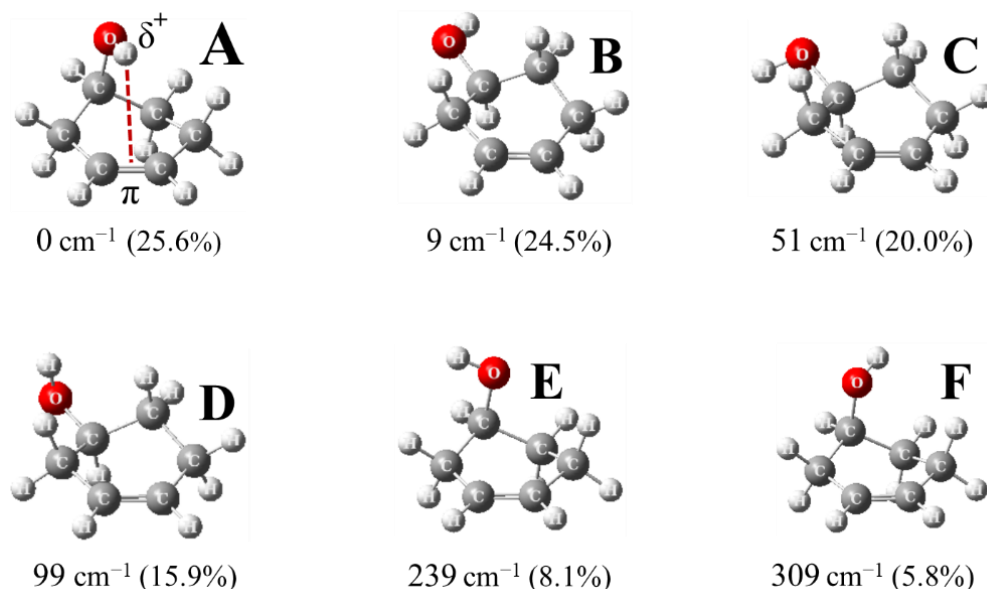
Conformers Labelled According to the CCSD(T)/aug-cc-pVTZ Calculated Energies							
							Reference
Ring-twisting angle (degrees)							
CCSD/cc-pVTZ	−29.3°	30.6°	−30.0°	30.1°	−30.8°	30.1°	This work
MP2/cc-pVTZ	−29.8°	31.6°	−30.6°	31.0°	−31.5°	31.0°	[51,54]
OH internal rotation angle (degrees)							
CCSD/cc-pVTZ	28.4°	46.8°	−55.9°	170.9°	173.2°	−74.9°	This work
MP2/cc-pVTZ	26.3°	45.7°	−51.7°	170.2°	173.1°	−74.6°	This work
Observed							
Vibrational frequencies (cm <sup>−1</sup> )							
OH stretch	3646	3632	3654	3649	3644	3650	[54]
C=C stretch	1652	1654	1657	1662	1662	1662	[54]

### 3.2.2. 3-Cyclohexen-1-ol (V)

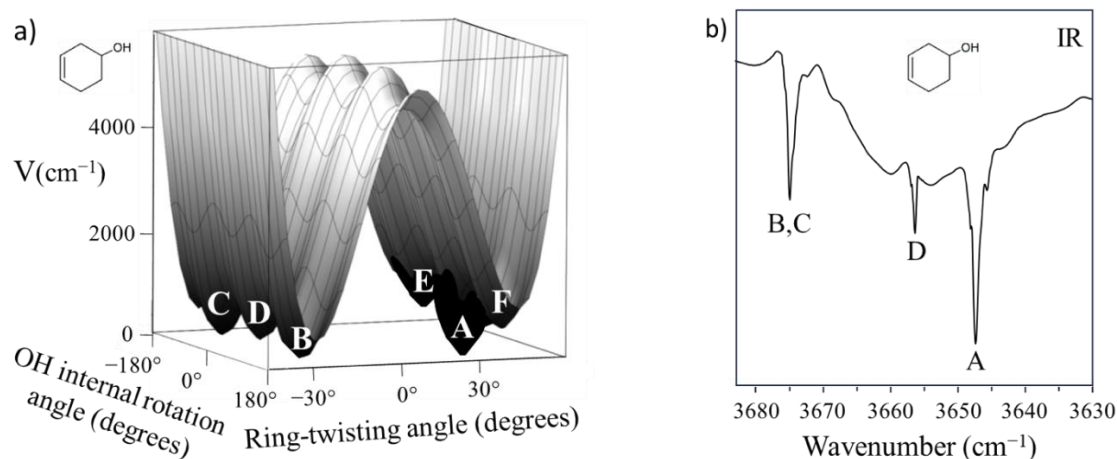
3-Cyclohexen-1-ol possesses six conformers which can interconvert into each other by ring-twisting and OH internal rotation. Figure 13 shows the calculated geometric structures of the conformers, and Figure 14a shows a calculated potential energy surface (PES) from MP2/cc-pVTZ computations for 3-cyclohexen-1-ol [55].

The lowest energy conformer of 3-cyclohexen-1-ol is **A**, and this lies 9 cm<sup>−1</sup> (0.03 kcal/mol) to 309 cm<sup>−1</sup> (0.88 kcal/mol) lower in energy than the other conformers according to CCSD(T)/aug-cc-pVTZ computations. This conformer has a calculated abundance of 25.6% in its vapor state at room temperature. Table 6 presents the calculated relative energies of 3-cyclohexen-1-ol from ab initio CCSD(T)/aug-cc-pVTZ, CCSD/cc-pVTZ and MP2/cc-pVTZ computations. This table also presents calculated geometrical structural parameters.

Table 6 and Figure 14b present the spectral data for this molecule. Conformer **A** has the strongest peak and lowest OH stretch frequency [55]. The calculated hydrogen bond O–H⋯ $\pi$  angle in degrees of conformer **A** is 112.0° from CCSD/cc-pVTZ and 113.6° from MP2/cc-pVTZ computations [55].

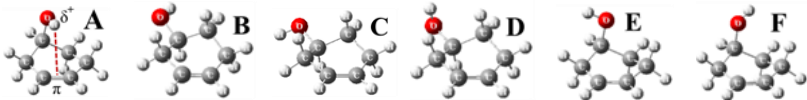


**Figure 13.** Calculated geometrical structures of the six conformers of 3-cyclohexen-1-ol from CCSD/cc-pVTZ computations. The relative energies and vapor-phase populations (in parentheses) at 25 °C are from CCSD(T)/aug-cc-pVTZ computations.



**Figure 14.** (a) Calculated PES from MP2/cc-pVTZ computations for 3-cyclohexen-1-ol. (b) Vapor-phase infrared spectrum at 164.5 °C in the OH stretching region.

**Table 6.** Calculated relative energies and selected geometrical structural parameters of the conformers of 3-cyclohexen-1-ol (V) and observed OH stretch vibrational frequencies in the vapor phase.

Conformers Labelled According to the CCSD(T)/aug-cc-pVTZ Calculated Energies							
							Reference
Method of calculation	Relative energy (cm <sup>-1</sup> )						
CCSD(T)/aug-cc-pVTZ	0	9	51	99	239	309	This work
CCSD/cc-pVTZ	10	0	35	82	235	277	[55]
MP2/cc-pVTZ	0	108	140	202	296	346	[55]
	Hydrogen atom on the oxygen distance to the center of the double bond (Å)						
CCSD/cc-pVTZ	2.614	4.511	4.313	4.153	3.539	3.832	[55]
MP2/cc-pVTZ	2.548	4.499	4.300	4.146	3.512	3.805	[55]
	Ring-twisting angle (degrees)						
CCSD/cc-pVTZ	30.0°	-30.3°	-30.4°	-30.0°	29.0°	28.4°	This work
MP2/cc-pVTZ	30.7°	-30.9°	-31.1°	-30.8°	29.8°	29.2°	[55]
	OH internal rotation angle (degrees)						
CCSD/cc-pVTZ	0.8°	155.7°	-90.6°	37.1°	-100.4°	131.1°	This work
MP2/cc-pVTZ	-0.1°	155.3°	-89.8°	37.8°	-100.4°	129.6°	[55]
Observed	Vibrational frequencies (cm <sup>-1</sup> )						
OH stretch	3647	3675	3675	3656	---	---	[55]

### 3.3. Unsaturated 3-Membered Ring Molecules with a Weak Intramolecular Hydrogen Bonding

#### 3.3.1. 2-Cyclopropen-1-ol (VI)

2-Cyclopropen-1-ol possesses three conformers which can interconvert into each other by OH internal rotation. Conformers **B1** and **B2** in Figure 15 are mirror images of each other. The conformer with lowest energy is **A**, and this lies 166 cm<sup>-1</sup> (0.47 kcal/mol) lower in energy than the other conformers according to CCSD(T)/aug-cc-pVTZ computations. This conformer has a calculated population of 52.7% in its vapor state at room temperature.

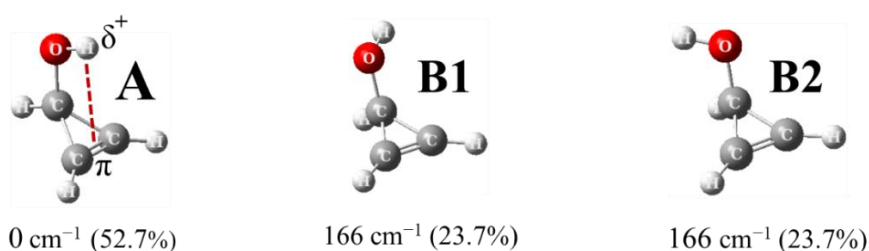


**Figure 15.** Calculated geometrical structures of the six conformers of 2-cyclopropen-1-ol from CCSD/cc-pVTZ computations. The indicated relative energies and estimated vapor phase population abundance at 25 °C per conformer are from CCSD(T)/aug-cc-pVTZ computations. The estimated relative population abundances are shown in parenthesis.

Table 7 presents the calculated relative energies of 2-cyclopropen-1-ol from ab initio CCSD(T)/aug-cc-pVTZ, CCSD/cc-pVTZ and MP2/cc-pVTZ computations. This table as well presents calculated selected geometrical structural parameters of 2-cyclopropen-1-ol. Conformer **A** is the only conformer of this molecule with the weak intramolecular O–H... $\pi$  hydrogen bond and has the lowest conformational energy.

**Table 7.** Calculated relative energies, selected geometrical structural parameters and OH and C=C stretching frequencies for the conformers of 2-cyclopropen-1-ol (VI).

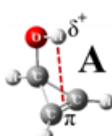


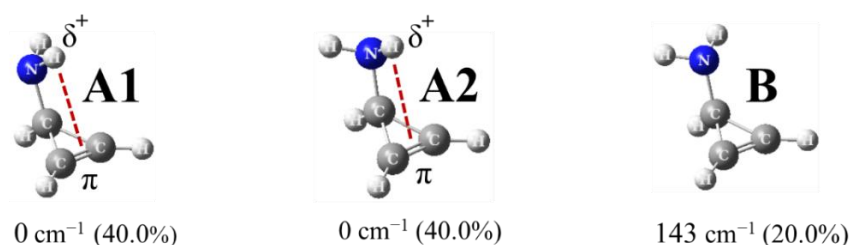
Conformers Labelled According to the CCSD(T)/aug-cc-pVTZ Calculated Energies				
				Reference
<u>Method of calculation</u>	Relative energy (cm <sup>-1</sup> )			
CCSD(T)/aug-cc-pVTZ	0	166	166	[This work]
CCSD/cc-pVTZ	0	171	171	[57]
MP2/cc-pVTZ	0	235	235	[57]
	Hydrogen on the oxygen distance to the center of the double bond (Å)			
CCSD/cc-pVTZ	2.488	3.018	3.018	[57]
MP2/cc-pVTZ	2.478	3.028	3.028	[57]
	OH internal rotation angle (degrees)			
CCSD/cc-pVTZ	0°	124.9°	−124.9°	[57]
MP2/cc-pVTZ	0°	127.9°	−127.9°	[57]
<u>Calculated</u>	Vibrational frequencies (cm <sup>-1</sup> )			
OH stretch	3643	3658	3658	[57]
C=C stretch	1600	1618	1618	[57]

Table 7 also shows the calculated O–H and C=C stretching frequencies for this molecule from MP2/cc-pVTZ computations [57]. Both are lowest for the  $\pi$  bonded conformer **A**. The calculated hydrogen bond O–H... $\pi$  angle in degrees of conformer **A** is 76.2° from CCSD/cc-pVTZ and 76.6° from MP2/cc-pVTZ computations.

### 3.3.2. 2-Cyclopropen-1-amine (VII)

2-Cyclopropen-1-amine possesses three conformers which can interconvert into each other by NH<sub>2</sub> internal rotation. The conformers **A1** and **A2** shown in Figure 16 are mirror images of each other and are of lowest conformational energy. **A1** and **A2** lie 143 cm<sup>-1</sup> (0.41 kcal/mol) lower in energy than conformer **B** according to CCSD(T)/aug-cc-pVTZ computations. This conformer has a calculated abundance of 40% in its vapor state at room temperature.

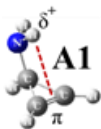
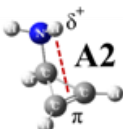
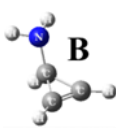


**Figure 16.** Calculated geometrical structures of the six conformers of 2-cyclopropen-1-amine from CCSD/cc-pVTZ computations. The relative energies and calculated vapor phase populations (in parentheses) at 25 °C for each conformer are from CCSD(T)/aug-cc-pVTZ computations.



Table 8 presents the calculated relative energies of 2-cyclopropen-1-amine from ab initio CCSD(T)/aug-cc-pVTZ, CCSD/cc-pVTZ and MP2/cc-pVTZ computations. This table in addition presents calculated selected geometrical structural parameters. Conformers **A1** and **A2** of 2-cyclopropen-1-amine possess a weak intramolecular N–H $\cdots\pi$  hydrogen bonds and these are responsible for the lowering of the conformational energy. Table 8 also presents the calculated frequencies for the NH<sub>2</sub> stretching and C=C stretching and the vibrations from MP2/cc-pVTZ computations [57]. The calculated hydrogen bond N–H $\cdots\pi$  angle in degrees is 73.4° from CCSD/cc-pVTZ and 73.6° from MP2/cc-pVTZ computations.

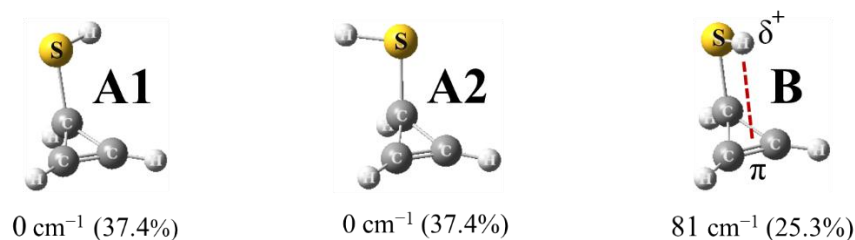
**Table 8.** Calculated relative energies, selected geometrical structural parameters and NH<sub>2</sub> and C=C stretch vibrational frequencies of the conformers of 2-cyclopropen-1-amine (VII).

Conformers Labelled According to the CCSD(T)/aug-cc-pVTZ Calculated Energies				
				Reference
Method of Calculation	Relative energy (cm <sup>-1</sup> )			
CCSD(T)/aug-cc-pVTZ	0	0	143	[This work]
CCSD/cc-pVTZ	0	0	118	[57]
MP2/cc-pVTZ	0	0	182	[57]
	Hydrogen atom on the nitrogen distance to the center of the double bond (Å)			
CCSD/cc-pVTZ <sup>a</sup>	2.583	3.147	3.112	[57]
MP2/cc-pVTZ <sup>a</sup>	2.571	3.147	3.106	[57]
CCSD/cc-pVTZ <sup>b</sup>	3.147	2.583	3.112	[57]
MP2/cc-pVTZ <sup>b</sup>	3.147	2.571	3.106	[57]
	NH <sub>2</sub> internal rotation angle (degrees)			
CCSD/cc-pVTZ	64.7°	−64.7°	180°	[57]
MP2/cc-pVTZ	65.6°	−65.6°	180°	[57]
Calculated	Vibrational frequencies (cm <sup>-1</sup> )			
NH <sub>2</sub> antisymmetric stretch	3414	3414	3406	[57]
NH <sub>2</sub> symmetric stretch	3345	3345	3346	[57]
C=C stretch	1607	1607	1636	[57]

<sup>a</sup> Distance of the “first” hydrogen of the amine group to the center of the C=C double bond. <sup>b</sup> Distance of the “second” hydrogen of the amine group to the center of the C=C double bond.

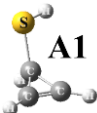
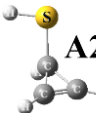
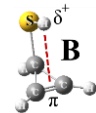
### 3.3.3. 2-Cyclopropen-1-thiol (IX)

2-Cyclopropen-1-thiol possesses three conformers which can interconvert into each other by SH internal rotation. Conformers **A1** and **A2** shown in Figure 17 are mirror images of each other, and these are of lowest energy. **A1** and **A2** lie 81 cm<sup>-1</sup> (0.23 kcal/mol) lower in energy than conformer **B** according to CCSD(T)/aug-cc-pVTZ computations. Conformer **B**, which is the conformation with the weak intramolecular S–H $\cdots\pi$  hydrogen bond, is not at the lowest energy. However, it has a lower calculated energy than would be expected without the  $\pi$ -type interaction [57]. Conformer **B** has a calculated abundance of 25% in its vapor state at room temperature. Table 9 presents the calculated relative energies of 2-cyclopropen-1-thiol from ab initio CCSD(T)/aug-cc-pVTZ, CCSD/cc-pVTZ and MP2/cc-pVTZ computations. This table also presents selected calculated geometrical structural parameters as well as the calculated vibrational frequencies for the S–H stretching and C=C stretching. Both vibrational frequencies are lowest for the  $\pi$  bonded conformer **B**. The calculated hydrogen bond S–H $\cdots\pi$  angle in degrees is 78.8° from CCSD/cc-pVTZ and 79.6° from MP2/cc-pVTZ computations.



**Figure 17.** Calculated geometrical structures of the six conformers of 2-cyclopropen-1-thiol from CCSD/cc-pVTZ computations. The relative energies and vapor-phase populations (in parentheses) at 25 °C are from CCSD(T)/aug-cc-pVTZ computations.

**Table 9.** Calculated relative energies, selected geometrical structural parameters and SH and C=C stretching frequencies for the conformers of the conformers of 2-cyclopropen-1-thiol (IX).

Conformers Labelled According to the CCSD(T)/aug-cc-pVTZ Calculated Energies				
	 A1	 A2	 B	Reference
<u>Method of Calculation</u>	Relative energy (cm <sup>-1</sup> )			
CCSD(T)/aug-cc-pVTZ	0	0	81	[This work]
CCSD/cc-pVTZ	0	0	110	[57]
MP2/cc-pVTZ	0	0	65	[57]
	Hydrogen atom on the sulfur distance to the center of the double bond (Å)			
CCSD/cc-pVTZ	3.450	3.450	2.774	[57]
MP2/cc-pVTZ	3.433	3.433	2.740	[57]
	SH internal rotation angle (degrees)			
CCSD/cc-pVTZ	118.9°	-118.9°	0°	[57]
MP2/cc-pVTZ	118.5°	-118.5°	0°	[57]
<u>Calculated</u>	Vibrational frequencies (cm <sup>-1</sup> )			
SH stretch	1338	1338	1337	[57]
C=C stretch	1636	1636	1614	[57]

#### 4. Discussion

In the present paper we have reported both experimental and theoretical results from previous studies, and we have refined this work with high level CCSD(T)/aug-cc-pVTZ computations. We believe that the CCSD(T)/aug-cc-pVTZ calculations for the relative energies are more reliable than our previous performed CCSD/cc-pVTZ and MP2/cc-pVTZ energy computations, and the discussion below is based on that assumption.

Our investigation of these nine molecules has painted a consistent picture showing that even though the  $\pi$ -type hydrogen bonding is weak, it is generally sufficiently strong enough to cause internal rotation, ring-puckering, and/or ring twisting to produce a lowest energy conformation that can accommodate its presence.

Of the molecules studied 3-cyclopenten-1-ol (I) and 2-indanol (II) possess the greatest conformational energy decreases through due to their  $\pi$  bonding. The conformations without the  $\pi$  bonding are 254 to 460 cm<sup>-1</sup> higher in energy. Their distances from the hydrogen atom on the oxygen to the  $\pi$  systems are approximately 2.4 Å, as compared to distances greater than 3.5 Å for the other conformers. The other five- and six-membered ring alcohols with  $\pi$  bonding studied have these distances in the 2.6 to 2.8 Å range. The small 2-cyclopropene-1-ol (VI) molecule has a distance of 2.5 Å from the O-H hydrogen atom to the C=C double bond.

The  $\pi$  bonded conformation of the 3-cyclopenten-1-amine (VII) has a conformational energy 128 to 200 cm<sup>-1</sup> lower than those without the  $\pi$  bond reflecting the fact that the N-H $\cdots\pi$ (C=C) interaction is weaker than the O-H $\cdots\pi$ (C=C) interaction. The S-H $\cdots\pi$ (C=C) interaction is weaker yet as the hydrogen bonding conformer is not of lowest energy.

The O-H stretching frequencies of the conformers with weak O-H $\cdots\pi$ (C=C) hydrogen bonds can be up to 32 cm<sup>-1</sup> lower than those of the non-hydrogen bonded cyclic alcohols as shown for 3-cyclopenten-1-ol, 2-cyclopenten-1-ol, 2-cyclohexen-ol and 3-cyclohexen-1-ol. For 2-cyclohexen-1-ol the second lowest energy conformer with a weak O-H $\cdots\pi$ (C=C) interaction has the lowest OH stretching frequency. For this molecule the most abundant conformer A has an intramolecular hydrogen bond with its O-H stretching frequency 14 cm<sup>-1</sup> higher

than conformer **B** and 2 cm<sup>-1</sup> higher than that of conformer E. The hydrogen bonded conformers of the cyclic alcohols studied possess C=C stretching frequencies up to 13 cm<sup>-1</sup> lower than those of the non-hydrogen bonded conformers. Supplementary Table S1 presents a numerical summary of these results.

From our experimental and theoretical results for 3-cyclopenten-1-amine (VII) we found that both the NH<sub>2</sub> antisymmetric stretching and the NH<sub>2</sub> symmetric stretching frequencies for the weak intramolecular N–H⋯π hydrogen bonded species **A1** and **A2** are 5 to 12 cm<sup>-1</sup> lower than those of the non-hydrogen bonded conformers. Supplementary Table S2 presents a numerical summary of these results.

According to our MP2/cc-pVTZ computations [57], the S–H⋯π(C=C) interaction slightly weakens the S–H bond of 2-cyclopropen-1-thiol. The lowering of the conformational energy due to the presence of the intramolecular weak S–H⋯π hydrogen bond is not enough to overcome other interactions and make the hydrogen bonded conformer the one with the lowest energy. The S–H and the C=C stretching frequencies of the hydrogen bonded conformer of this molecule are lower by 1 cm<sup>-1</sup> and by 22 cm<sup>-1</sup>, respectively, than those of the non-hydrogen bonded conformers. Supplementary Table S3 presents a numerical summary of these results along with calculated results for 2-cyclopropen-1-ol and 2-cyclopropen-1-amine.

## 5. Conclusions

The combination of theoretical computations with IR and Raman spectroscopy has proven to be an invaluable tool for the investigation of weakly π bonding conformers of molecules in their vapor states. Weak π-type intramolecular hydrogen bonding lowers the conformational energy for small cyclic molecules. For all of the molecules studied, with the exception of 2-cyclopropen-1-thiol, the lowest energy conformer possesses an intramolecular hydrogen bond. Cyclic alcohols are capable of forming stronger intramolecular π-type hydrogen bonds than cyclic amines or cyclic thiols according to the electronegativity of the heteroatom.

## Supplementary Materials

The additional data and information can be downloaded at: <https://media.sciltp.com/articles/others/2510201115283390/Supplementary-Material-for-final.pdf>. Supplementary Table S1 presents a summary of the calculated CCSD(T)/aug-cc-pVTZ energies (cm<sup>-1</sup>) and observed OH and C=C stretching frequencies for the cyclic alcohols. Supplementary Table S2 presents a summary of the calculated CCSD(T)/aug-cc-pVTZ energies (cm<sup>-1</sup>) and observed NH<sub>2</sub> and C=C stretching frequencies for 3-cyclopenten-1-amine and Supplementary Table S3 presents a summary of the calculated CCSD(T)/aug-cc-pVTZ energies (cm<sup>-1</sup>) and calculated OH, NH<sub>2</sub> and C=C stretching frequencies for 2-cyclopropen-1-ol, 2-cyclopropen-1-amine and 2-cyclopropen-1-thiol.

## Author Contributions

E.J.O. recorded the IR and Raman spectra, performed ab-initio computations, and elaborated the tables and illustrations. E.J.O. and J.L. contributed equally to the text of the article. All authors have read and agreed to the published version of the manuscript.

## Funding

This research received no external funding.

## Institutional Review Board Statement

Not applicable.

## Informed Consent Statement

Not applicable.

## Acknowledgments

The authors congratulate Rui Fausto for launching this new journal and wish him and the journal great success. The authors also congratulate Gus Zerbi for his many outstanding contributions to the spectroscopic community. E.J.O. and J. L. thank the advanced computing resources provided by Texas A&M High Performance Research Computing, and the Laboratory for Molecular Simulation at Texas A&M University, College Station for the Gaussian16 computational resource. We also thank the Welch Foundation for the financial support provided for our previous work on hydrogen bonding.

## Conflicts of Interest

The authors declare no conflict of interest.

## Use of AI and AI-Assisted Technologies

No AI tools were utilized for this paper.

## References

1. Jeffrey, G.A.; Saenger, W. *Hydrogen Bonding in Biological Structures*, 2nd ed.; Springer: Berlin/Heidelberg, Germany, 1991.
2. Jeffrey, G.A. *An Introduction to Hydrogen Bonding*; Oxford University Press: New York, NY, USA, 1997.
3. Kojić-Prodić, B.K.; Molčanov, K. The Nature of Hydrogen Bond: New Insights into Old Theories. *Acta Chim. Slov.* **2008**, *55*, 692–708.
4. Zhyganiuk, I.V.; Malomuzh, M.P. Physical Nature of Hydrogen Bond. *Ukr. J. Phys.* **2015**, *60*, 960–974.
5. Grabowski, S.J. (Ed.) *Hydrogen Bonding—New Insights*, 1st ed.; Springer: Dordrecht, The Netherlands, 2006.
6. Desiraju, G.R.; Steiner, T. *The Weak Hydrogen Bond in Structural Chemistry and Biology*, 1st ed.; Oxford University Press: New York, NY, USA, 1998; Reprinted 2001.
7. Gilli, G.; Gilli, P. *The Nature of the Hydrogen Bond—Outline of a Comprehensive Hydrogen Bond Theory*, 1st ed.; Oxford University Press: New York, NY, USA, 2009.
8. Steiner, T.; Koellner, G. Hydrogen Bonds with  $\pi$ -Acceptors in Proteins: Frequencies and Role in Stabilizing Local 3D Structures. *J. Mol. Biol.* **2001**, *305*, 535–557.
9. Meyer, E.A.; Castellano, R.K.; Diederich, F. Interactions with Aromatic Rings in Chemical and Biological Recognition. *Angew. Chem. Int. Ed. Engl.* **2003**, *42*, 1210–1250.
10. Liaquat, H.; Imran, M.; Saddique, Z.; et al. Exploring the Versatility of Hydrogen-Bonded Organic Frameworks: Advances in Design, Stability, and Multifunctional Applications. *J. Mol. Struct.* **2025**, *1321*, 140221.
11. Elewa, A.M. Hydrogen-Bonded Organic Frameworks (HOFs) from Design to Environmental Application. *J. Ind. Eng. Chem.* **2025**, *145*, 169–190.
12. Takasashi, O.; Kohno, Y.; Nishio, M. Relevance of Weak Hydrogen Bonds in the Conformation of Organic Compounds and Bioconjugates: Evidence from Recent Experimental Data and High-Level ab Initio MO Calculations. *Chem. Rev.* **2010**, *110*, 6049–6076.
13. Salonen, L.M.; Ellermann, M.; Diederich, F. Aromatic Rings in Chemical and Biological Recognition: Energetics and Structures. *Angew. Chem. Int. Ed. Engl.* **2011**, *50*, 4808–4842.
14. Arkas, M.; Kitsou, O.; Gkouma, A.; et al. The Role of Hydrogen Bonds in the Mesomorphic Behaviour of Supramolecular Assemblies Organized in Dendritic Architectures. *Liq. Cryst. Rev.* **2019**, *7*, 60–105.
15. Bu, R.; Xiong, Y.; Wei, X.; et al. Hydrogen Bonding in CHON-Containing Energetic Crystals: A Review. *Cryst. Growth Des.* **2019**, *19*, 5981–5997.
16. Juhaš, M.; Zitko, J. Molecular Interactions of Pyrazine-Based Compounds to Proteins. *J. Med. Chem.* **2020**, *63*, 8901–8916.
17. Liu, A.; Zhou, Y.; Yuan, L. Hydrogen-Bonded Aromatic Amide Macrocycles: Synthesis, Properties and Functions. *Org. Biomol. Chem.* **2022**, *20*, 9023–9051.
18. Samuel, H.S.; Nweke-Maraizu, U.; Etim, E.E. Understanding Intermolecular and Intramolecular Hydrogen Bonds: Spectroscopic and Computational Approaches. *J. Chem. Rev.* **2023**, *5*, 439–465.
19. Haque, A.; Alenezi, K.M.; Khan, M.S.; et al. Non-Covalent Interactions (NCIs) In  $\pi$ -Conjugated Functional Materials: Advances and Perspectives. *Chem. Soc. Rev.* **2023**, *52*, 454–472.
20. Lin, L.; Jones, T.W.; Yang, T.C.J.; et al. Hydrogen Bonding in Perovskite Solar Cells. *Matter* **2024**, *7*, 38–58.
21. Grabowski, S.J. Hydrogen Bond Types Which do not fit Accepted Definitions. *Chem. Commun.* **2024**, *60*, 6239–6255.

22. Rao, C.N.R.; Murthy, A.S.N. Spectroscopic Studies of Hydrogen Bonding. In *Developments in Applied Spectroscopy*; Grove, E.L., Perkins, A.J., Eds.; Springer: Boston, MA, USA, 1970; Volume 7b, pp. 54–88.
23. Møllendal, H. Recent Gas-Phase Studies of Intramolecular Hydrogen Bonding. In *Structures and Conformations of Non-Rigid Molecules, NATO ASI Series, Series C: Mathematical and Physical Science*; Laane, J., Dakkouri, M., van der Veken, B., et al., Eds.; Springer Science + Business Media, B.V.: Dordrecht, The Netherlands, 1993; Volume 410, pp. 277–301.
24. Kovács, A.; Szabó, A.; Hargittai, I. Structural Characteristics of Intramolecular Hydrogen Bonding in Benzene Derivatives. *Acc. Chem. Res.* **2002**, *35*, 887–894.
25. Lyssenko, K.A.; Antipin, M.Y. The Nature and Energy Characteristics of Intramolecular Hydrogen Bonds in crystals. *Russ. Chem. Bull.* **2006**, *55*, 1–15.
26. Sobczyk, L.; Chudoba, D.; Tolstoy, P.M.; et al. Some Brief Notes on Theoretical and Experimental Investigations of Intramolecular Hydrogen Bonding. *Molecules* **2016**, *21*, 1657.
27. Hansen, P.E.; Spanget-Larsen, J. NMR and IR Investigations of Strong Intramolecular Hydrogen Bonds. *Molecules* **2017**, *22*, 552.
28. Caron, G.; Vallaro, M.; Ermondi, G. High Throughput Methods to Measure the Propensity of Compounds to form Intramolecular Hydrogen Bonding. *Med. Chem. Commun.* **2017**, *8*, 1143–1151.
29. Jezierska, A.; Tolstoy, P.M.; Panek, J.J.; et al. Intramolecular Hydrogen Bonds in Selected Aromatic Compounds: Recent Developments. *Catalysts* **2019**, *9*, 909.
30. Caron, G.; Kihlberg, J.; Ermondi, G. Intramolecular Hydrogen Bonding: An Opportunity for Improved Design in Medicinal Chemistry. *Med. Res. Rev.* **2019**, *39*, 1707–1729.
31. Deshmukh, M.M.; Gadre, S.R. Molecular Tailoring Approach for the Estimation of Intramolecular Hydrogen Bond Energy. *Molecules* **2021**, *26*, 2928.
32. Hansen, P.E. A Spectroscopic Overview of Intramolecular Hydrogen Bonds of NH...O, S, N Type. *Molecules* **2021**, *26*, 2409.
33. Hakobyan, R.M.; Shahkhatuni, A.G.; Polynski, M.V.; et al. The Role of the Nitro Group on the Formation of Intramolecular Hydrogen Bond in the Methyl Esters of 1-Vinyl-nitro-pyrazolecarboxylic Acids. *J. Mol. Struct.* **2025**, *1322*, 140350.
34. Rouquet, E.; Dupont, J.; Vincent, J.; et al. The Role of Intramolecular Hydrogen Bonding in Photoelectron Circular Dichroism: The Diastereoisomers of 1-Amino-2-Indanol. *Phys. Chem. Chem. Phys.* **2025**, *27*, 2739–2748.
35. Baker, A.W.; Shulgin, A.T. Intramolecular Hydrogen Bonds to  $\pi$ -Electrons and Other Weakly Basic Group. *J. Am. Chem. Soc.* **1958**, *80*, 5358–5363.
36. Morokuma, K.; Wipff, G. Theoretical Evidence for Intramolecular Hydrogen Bonding in 7-Norbornenol. *Chem. Phys. Lett.* **1980**, *74*, 400–403.
37. Smith, Z.; Carballo, N.; Wilson, E.B.; et al. Conformations, Possible Hydrogen Bonding, and Microwave Spectrum of 3-Buten-2-ol. *J. Am. Chem. Soc.* **1985**, *107*, 1951–1957.
38. Bakke, J.M.; Schie, A.M.; Skjetne, T. Conformation of Allylic Alcohols and Intramolecular Hydrogen Bonding. *Acta Chem. Scand. B* **1986**, *40*, 703–710.
39. Marstokk, K.-M.; Møllendal, H. Microwave Spectrum, Conformation and Intramolecular Hydrogen Bonding of 1,4-Pentadien-3-ol. *Acta Chem. Scand.* **1990**, *44*, 18–22.
40. Marstokk, K.-M.; Møllendal, H.; Samdal, S. Microwave Spectrum, Conformation and Intramolecular Hydrogen Bonding of 1-Mercapto-2-propanol. *Acta Chem. Scand.* **1990**, *44*, 339–345.
41. Melandri, S.; Favero, P.G.; Caminati, W. Detection of the *syn* Conformer of Allyl Alcohol by Free Jet Microwave Spectroscopy. *Chem. Phys. Lett.* **1994**, *223*, 541–545.
42. Bräse, S.; Klæboe, P.; Marstokk, K.-M.; et al. Conformational Properties of 2-Cyclopropylideneethanol as Studied by Microwave, Infrared and Raman Spectroscopy and by Ab Initio Computations. *Acta Chem. Scand.* **1998**, *52*, 1122–1136.
43. Leonov, A.; Marstokk, K.-M.; de Meijere, A.; et al. Microwave Spectrum, Conformational Equilibrium, Intramolecular Hydrogen Bonding, Tunneling and Quantum Chemical Calculations for 1-Ethenylcyclopropan-1-ol. *J. Phys. Chem. A* **2000**, *104*, 4421–4428.
44. Rademacher, P.; Khelashvili, L.; Kowski, K. Spectroscopic and Theoretical Studies on Intramolecular OH $\cdots\pi$  Hydrogen Bonding in 4-Substituted 2-Allylphenols. *Org. Biomol. Chem.* **2005**, *3*, 2620–2625.
45. Isozaki, T.; Tsutsumi, Y.; Suzuki, T.; et al. Direct Evidence for Weak Intramolecular O–H $\cdots\pi$  Hydrogen Bonding in 1-Hydroxytetralin. *Chem. Phys. Lett.* **2010**, *495*, 175–178.
46. Miller, B.J.; Lane, J.R.; Kjaergaard, H.G. Intramolecular OH $\cdots\pi$  Interactions in Alkenols and Alkynols. *Phys. Chem. Chem. Phys.* **2011**, *13*, 14183–14193.
47. Mackeprang, K.; Schröder, S.D.; Kjaergaard, H.G. Weak Intramolecular OH $\cdots\pi$  Hydrogen Bonding in Methallyl- and Allyl-Carbinol. *Chem. Phys. Lett.* **2013**, *582*, 31–37.



48. Das, P.; Das, P.K.; Arunan, E. Conformational Stability and Intramolecular Hydrogen Bonding in 1,2-Ethanediol and 1,4-Butanediol. *J. Phys. Chem. A* **2015**, *119*, 3710–3720.
49. Al-Saadi, A.A.; Ocola, E.J.; Laane, J. Intramolecular  $\pi$ -Type Hydrogen Bonding and Conformations of 3-Cyclopenten-1-ol. 1. Theoretical Calculations. *J. Phys. Chem. A* **2010**, *114*, 7453–7456.
50. Ocola, E.J.; Al-Saadi, A.A.; Mlynek, C.; et al. Intramolecular  $\pi$ -Type Hydrogen Bonding and Conformations of 3-Cyclopenten-1-ol. 2. Infrared and Raman Spectral Studies at High Temperatures. *J. Phys. Chem. A* **2010**, *114*, 7457–7461.
51. Ocola, E.J. Vibrational and Theoretical Investigations of Molecular Conformations and Intramolecular  $\pi$ -Type Hydrogen Bonding. Ph. D. Thesis, Texas A & M University, College Station, TX, USA, 2011.
52. Al-Saadi, A.A.; Wagner, M.; Laane, J. Spectroscopic and Computational Studies of the Intramolecular Hydrogen Bonding of 2-Indanol. *J. Phys. Chem. A* **2006**, *110*, 12292–12297.
53. Ocola, E.J.; Laane, J. Spectroscopic and Theoretical Study of the Intramolecular  $\pi$ -Type Hydrogen Bonding and Conformations of 2-Cyclopenten-1-ol. *Molecules* **2021**, *26*, 1106.
54. Ocola, E.J.; Laane, J. Spectroscopic and Theoretical Study of the Intramolecular  $\pi$ -Type Hydrogen Bonding and Conformations of 2-Cyclohexen-1-ol. *J. Phys. Chem. A* **2016**, *120*, 74–80.
55. Ocola, E.J.; Laane, J. Spectroscopic and Theoretical Study of the Intramolecular  $\pi$ -Type Hydrogen Bonding and Conformations of 3-Cyclohexen-1-ol. *J. Mol. Spectrosc.* **2022**, *387*, 111663.
56. Laane, J.; Ocola, E.J.; Chun, H.J. Vibrational Potential Energy Surfaces in Ground and Excited Electronic States. In *Frontiers and Advances in Molecular Spectroscopy*, 1st ed.; Laane, J., Ed.; Elsevier Publishing: Amsterdam, The Netherlands, 2017; Chapter 4, pp. 101–142.
57. Ocola, E.J.; Laane, J. Theoretical Investigation of Intramolecular  $\pi$ -Type Hydrogen Bonding and Internal Rotation of 2-Cyclopropen-1-ol, 2-Cyclopropen-1-thiol and 2-Cyclopropen-1-amine. *Mol. Phys.* **2018**, *17*, 1404–1412.
58. Varfolomeeva, V.V.; Terentev, A.V. Weak Intramolecular and Intermolecular Hydrogen Bonding of Benzyl Alcohol, 2-Phenylethanol and 2-Phenylethylamine in the Adsorption on Graphitized Thermal Carbon Black. *Phys. Chem. Chem. Phys.*, **2015**, *17*, 24282–24293.
59. Ocola, E.J.; Laane, J. Spectroscopic and Theoretical Study of the Intramolecular  $\pi$ -Type Hydrogen Bonding and Conformations of 3-Cyclopentene-1-amine. *J. Phys. Chem. A* **2020**, *124*, 5907–5916.
60. Marstokk, K.-M.; Møllendal, H. Microwave Spectrum, Conformation and Internal Hydrogen Bonding in N-Methylallylamine. *Acta Chem. Scand. A* **1986**, *40*, 615–621.
61. Marstokk, K.-M.; Møllendal, H. Microwave Spectra and Weak Intramolecular Hydrogen Bonding in 3-Butene-1-Thiol And N-Methylallylamine. In *Structure and Dynamics of Weakly Bound Molecular Complexes, NATO ASI Series, Series C: Mathematical and Physical Science*; Weber, A., Ed.; Springer Science + Business Media, B.V.: Dordrecht, The Netherlands, 1993; Volume 212, pp. 57–68.
62. Marstokk, K.-M.; Møllendal, H. Microwave Spectrum, Conformational Equilibria and Intramolecular Hydrogen Bonding of 1-Amino-3-butene. *Acta Chem. Scand. A* **1988**, *42*, 374–390.
63. Marstokk, K.-M.; de Meijere, A.; Møllendal, H.; et al. Microwave Spectrum, Conformation, Dipole Moment and Quantum Chemical Calculations of 1-Amino-1-ethenylcyclopropane. *J. Phys. Chem. A* **2000**, *104*, 2897–2901.
64. Sastry, K.V.L.N.; Dass, S.C.; Brooks, W.V.F.; et al. Microwave Spectrum, Dipole Moment, and Molecular Structure of Allyl Mercaptan. *J. Mol. Spect.* **1969**, *31*, 54–65.
65. Marstokk, K.-M.; Møllendal, H. Microwave Spectrum, Conformational Equilibria, Intramolecular Hydrogen Bonding and Centrifugal Distortion of 3-Butene-1-thiol. *Acta Chem. Scand.* **1986**, *40*, 402–411.
66. Laane, J. One-dimensional potential energy functions in vibrational spectroscopy. *Q. Rev. Chem. Soc.* **1971**, *25*, 533–552.
67. Laane, J. Determination of Vibrational Potential Energy Surfaces from Raman and Infrared Spectra. *Pure Appl. Chem.* **1987**, *59*, 1307–1326.
68. Laane, J. Vibrational Potential Energy Surfaces of Non-Rigid Molecules in Ground and Excited Electronic States. In *Structures and Conformations of Non-Rigid Molecules, NATO ASI Series, Series C: Mathematical and Physical Science*; Laane, J., Dakkouri, M., van der Veken, B., et al., Eds.; Springer Science + Business Media B.V.: Dordrecht, The Netherlands, 1993; Volume 410, 65–98.
69. Laane, J. Vibrational Potential Energy Surfaces and Conformations of Molecules in Ground and Excited Electronic States. *Annu. Rev. Phys. Chem.* **1994**, *45*, 179–211.
70. Laane, J. Spectroscopic Determination of Ground and Excited State Vibrational Potential Energy Surfaces. *Int. Rev. Phys. Chem.* **1999**, *18*, 301–341.
71. Laane, J. Vibrational Potential Energy Surfaces of Non-Rigid Molecules in Excited Electronic States. In *Structure and Dynamics of Electronic Excited States*; Laane, J., Takahashi, H., Bandrauk, A., Eds.; Springer: Berlin, Germany, 1999; pp. 3–35.

72. Laane, J. Experimental Determination of Vibrational Potential Energy Surfaces and Molecular Structures in Electronic Excited States. *J. Chem. Phys. A* **2000**, *104*, 7715–7733.
73. Laane, J. Vibrational Potential Energy Surfaces in Electronic Excited States. In *Frontiers of Molecular Spectroscopy*, 1st ed.; Laane, J., Ed.; Elsevier Inc.: Amsterdam, The Netherlands, 2009; pp. 63–132.
74. Ocola, E.J.; Laane, J. Beyond the Harmonic Oscillator; Highlights of Selected Studies of Vibrational Potential Energy Functions. *Molecules* **2025**, *30*, 1492.
75. Frisch, M.J.; Trucks, G.W.; Schlegel, H.B.; et al. *Gaussian 16 (Revision B.01)*; Gaussian Inc.: Wallingford, CT, USA, 2016.
76. Dennington, R.D., II; Keith, T.A.; Millam, J.M. *GaussView (6.1.1), Graphical Interface*; Semichem Inc.: Shawnee, KS, USA, 2000–2019.
77. *Maple (2015, 2019.2)*; Maplesoft, a Division of Waterloo Maple Inc.: Waterloo, ON, Canada, 2015.
78. Haller, K.; Chiang, W.-Y.; del Rosario, A.; et al. High-Temperature Vapor-Phase Raman Spectra and Assignment of the Low-Frequency Modes of trans-Stilbene and 4-Methoxy-trans-Stilbene. *J. Mol. Struct.* **1996**, *379*, 19–23.
79. Laane, J.; Haller, K.; Sakurai, S.; et al. Raman Spectroscopy of Vapors at Elevated Temperatures. *J. Mol. Struct.* **2003**, *650*, 57–68.